Locomotor function of the dorsal fin in rainbow trout: kinematic patterns and hydrodynamic forces

The Journal of Experimental Biology 208, 4479-4494
Published by The Company of Biologists 2005
doi:10.1242/jeb.01922

Locomotor function of the dorsal fin in rainbow trout: kinematic patterns and hydrodynamic forces

Eliot G. Drucker[1] and George V. Lauder[2,*]

[1]*Washington Trout, PO Box 402, Duvall, WA 98019, USA* and [2]*Museum of Comparative Zoology, Harvard University, 26 Oxford Street, Cambridge, MA 02138, USA*

*Author for correspondence (e-mail: glauder@oeb.harvard.edu)

Accepted 4 October 2005

Summary

In this study, we examine the kinematics and hydrodynamics of the soft dorsal fin in a representative basal teleost, the rainbow trout (*Oncorhynchus mykiss*), during steady rectilinear locomotion at 0.5–2.0 body lengths (L) s^{-1} and during maneuvering. During steady swimming, dorsal fin height and sweep amplitude decrease with increasing speed. The dorsal fin wake, as viewed within a horizontal plane, consists of paired vortices on each side of the body (0.5 L s^{-1}) or nearly linearly arrayed vortex centers above the body (1.0 L s^{-1}) with central jet flows directed predominately laterally (lateral:thrust force ratio=5–6). At 2.0 L s^{-1}, the dorsal fin is no longer recruited to add momentum to the wake. This pattern of decreasing involvement of the trout dorsal fin in thrust production with increasing speed contrasts with the results of our previous study of the soft dorsal fin of sunfish (*Lepomis*), which is hydrodynamically inactive at low speed and sheds a propulsive vortex wake at higher speed. Yawing maneuvers by trout involve unilateral production of a single vortex ring by the dorsal fin with a strong jet flow oriented almost directly laterally. During steady swimming, interception by the tail of the dorsal fin's vortical wake and the adipose fin's non-vortical (drag) wake is hypothesized as a mechanism for enhancing tail thrust. This study provides the first experimental evidence that the plesiomorphic soft dorsal fin of ray-finned fishes acts as an ancillary force generator during axial locomotion. We suggest that the distinction often made between median and paired fin (MPF) propulsion and body and caudal fin (BCF) propulsion in fishes obscures the important role of multiple propulsors acting in a coordinated fashion. Using a combination of anterior median fin oscillation and axial undulation, without continuous paired fin excursions, trout employ an 'M–BCF' gait during steady swimming. The primarily lateral orientation of dorsal fin force in trout induces corresponding roll and yaw moments, which must be countered by forces from the caudal, anal and paired fins. Locomotion in trout therefore involves the simultaneous active use of multiple fins, presumably to maintain body stability in the face of environmental perturbations.

Key words: swimming, maneuvering, locomotion, dorsal fin, adipose fin, vortex wake, flow visualization, digital particle image velocimetry, rainbow trout, *Oncorhynchus mykiss*.

Introduction

A key feature of locomotor anatomy in fishes is the dorsal fin, which is one of three median fins, together with the anal and caudal fin, present in most species (Helfman et al., 1997; Lauder et al., 2002; Standen and Lauder, 2005). The dorsal fin displays considerable diversity in structure among ray-finned fishes. The plesiomorphic condition consists of a single 'soft' fin supported by flexible, segmented fin rays, while the derived dorsal fin in the spiny-finned acanthomorph fishes is composed of an anterior dorsal fin with stiff fin spines as supports and a posterior soft-rayed dorsal fin homologous to that in basal clades (Fig. 1; Lauder and Drucker, 2004; Mabee et al., 2002). While anatomical differences between spiny and soft dorsal fins have been well documented and a number of hypothesized locomotor functions of dorsal fins have been presented (Gosline, 1971; Lauder, 2005), as yet the dorsal fin of fishes has been the subject of limited experimental study compared with other propulsor systems such as the caudal fin and the paired pectoral fins.

Previous work examining the role of the dorsal fin in fish swimming has been concerned primarily with documentation of patterns of fin motion and theoretical modeling of fin forces. This research has focused on several relatively small teleostean clades exhibiting specialized swimming modes in which the dorsal fin is employed as a key propulsor. Particular attention has been given to fishes of the orders Tetraodontiformes (e.g. triggerfishes and boxfishes) and Gasterosteiformes (e.g. seahorses). These fishes swim steadily by undulating or oscillating the dorsal fin, usually in concert with other median fin surfaces (Arreola and Westneat, 1996; Breder and Edgerton, 1942; Consi et al., 2001; Gordon et al., 2000; Harris,

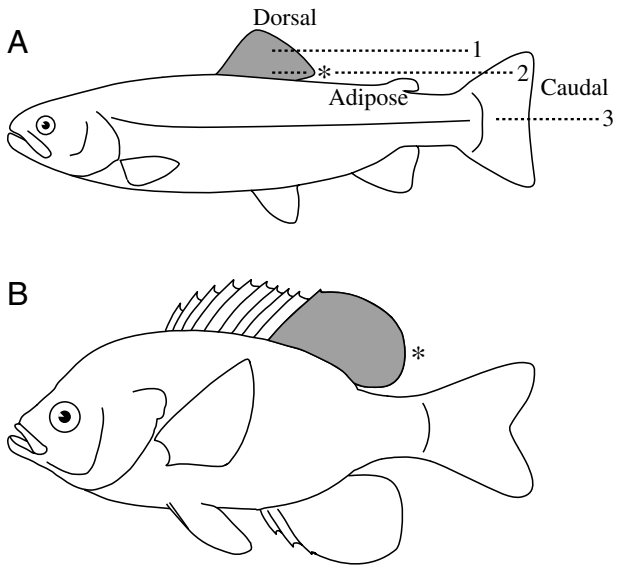

Fig. 1. (A) Rainbow trout, *Oncorhynchus mykiss*, shown with the three laser plane positions used to image flow in the wake of the dorsal and caudal fins. Note the small adipose fin, common to salmoniform fishes, located in the midline between the dorsal fin and the tail. Unlike other median fins, the adipose fin does not possess intrinsic musculature or skeletal supports. Plane 1, located at mid-dorsal fin height, was used to image wake flow patterns produced by the dorsal fin alone. At this position, the light sheet was sufficiently distant from the dorsal surface of the trout's body that dorsal-fin wake flow patterns could be calculated without interference from body flows. Plane 2 intersected both the trailing edge of the dorsal fin and the dorsal lobe of the tail. This plane was used to quantify wake patterns from the lower portion of the dorsal fin and to quantify movement of the tail through the dorsal fin wake. This position also permitted occasional observation of adipose-fin wake flow patterns when trout moved slightly upward, bringing the adipose fin within the light sheet. Plane 3, located at the tail mid-fork position, was used to image the wake shed by the body and caudal fin alone. Laser planes 1–3 were similar in relative position to those used by Drucker and Lauder (2001a) in their study of sunfish dorsal fin function. (B) Sunfish, *Lepomis macrochirus*, scaled to the same body length as the trout in A, showing differences in dorsal fin morphology, placement and relative size. The spiny dorsal fin (absent in trout) is anterior to the soft dorsal fin, which is shaded gray in both species. Both the relative area of the soft dorsal fin and the portion of the fin's trailing edge that extends posteriorly free from the body (marked by asterisks) are smaller in trout than in sunfish. As a result, the trailing edge of the soft dorsal fin is considerably closer to the leading edge of the tail in sunfish than in trout.

1937; Hove et al., 2001; Korsmeyer et al., 2002). The hydromechanical role of these dorsal fin motions (i.e. in producing locomotor forces) has been explored through mathematical modeling (Blake, 1976, 1977, 1978; Lighthill and Blake, 1990; Wright, 2000). Study of dorsal fin locomotion in other teleosts has had a similar primary taxonomic focus on acanthomorph fishes (Drucker and Lauder, 2001a; Jayne et al., 1996; Lindsey, 1978; Standen and Lauder, 2005).

In spite of these contributions, data on dorsal fin function in swimming fishes remain scarce in three important areas. First, there is little information about patterns of dorsal fin use during steady locomotion at different speeds and during unsteady maneuvering locomotion (Drucker and Lauder, 2001a; Standen and Lauder, 2005), and synchronized kinematic and electromyographic data are available for only one teleost species (Jayne et al., 1996). Second, we lack empirical hydrodynamic analyses of dorsal fin function based on experimental investigation of wake momentum flows. Such an approach is critical to understanding the functional significance of dorsal fin design in fishes. Third, our knowledge of dorsal fin mechanics in basal teleost fishes with soft dorsal fins is extremely limited. Previous work on these clades has focused on morphologically specialized taxa with highly elongate dorsal fins and with other fins absent or much reduced, such as certain osteoglossomorph, elopomorph and anguilliform fishes (Blake, 1980; Lindsey, 1978; Lissmann, 1961). We are aware of no prior empirical study of dorsal fin hydrodynamic function in a teleost fish possessing generalized soft dorsal fin anatomy.

In this paper, we conduct an experimental hydrodynamic analysis of dorsal fin function in a representative teleost with a soft dorsal fin, the rainbow trout (*Oncorhynchus mykiss*), through the use of quantitative wake flow visualization. Salmoniform fishes, including trout and salmon, are well known for high-speed, long-distance swimming powered by body and caudal fin (BCF) undulation (Webb, 1984), yet little is known about the role of non-BCF propulsion in this major taxonomic group. The function of the paired pectoral fins during locomotion in *O. mykiss* was examined recently by Drucker and Lauder (2003); median fins other than the tail have been studied in salmonids primarily in the context of non-locomotor function such as territorial display (Kalleberg, 1958; Keenleyside and Yamamoto, 1962). The primary goal of the present paper is to characterize how the dorsal fin in trout is recruited as an ancillary propulsor during axial locomotion and the extent to which the fin generates propulsive fluid forces. Specifically, we first describe the kinematics and wake dynamics of the dorsal fin during steady swimming over a range of speeds and during unsteady turning maneuvers. Second, we evaluate a previously untested hypothesis in the literature concerning the functional role of the basal teleost soft dorsal fin in generating thrust and lateral stabilizing forces. Finally, we examine hydrodynamic interactions between the tail and the wake shed by the dorsal fin to assess the possibility that multiple median fins oscillating in tandem can affect overall propulsive efficiency.

We interpret our results from trout in the light of an earlier study (Drucker and Lauder, 2001a) that initiated experimental hydrodynamic study of dorsal fin function in bluegill sunfish (*Lepomis macrochirus*) and a previous three-dimensional kinematic analysis of median fin function in sunfish (Standen and Lauder, 2005). Through a comparison of representative basal and derived teleosts, we seek to document variation in function of the soft-rayed dorsal fin, the plesiomorphic portion of the fin retained throughout teleost fish evolution.

Materials and methods

Fish

Rainbow trout [*Oncorhynchus mykiss* (Walbaum 1792)] were obtained from Red-Wing Meadow Hatchery, Montague, MA, USA and housed in circular 1200 liter tanks at 15°C. Animals were fed a maintenance ration of commercial trout pellets three times each week and acclimated to laboratory conditions for two weeks before experimentation. Trout were lightly anesthetized using tricaine methanesulfonate (MS-222) to allow morphological measurement of the dorsal fin. Digital photographs were taken of fish in left lateral aspect, from which surface area of the fully expanded dorsal fin was measured using ImageJ software (National Institutes of Health, USA). Nine animals of similar size (total body length, L, 19.6±0.7 cm, mean ± S.D.) were selected for swimming trials, which were conducted at 15°C.

Behavioral observations and wake visualization

Trout swam individually in the center of the working area (28 cm×28 cm×80 cm) of a temperature-controlled variable-speed freshwater flow tank (600 liters) under conditions similar to those described in our previous research on salmonids (Drucker and Lauder, 2003; Liao et al., 2003a,b; Nauen and Lauder, 2002b). The swimming behaviors induced were directly comparable with those characterized in our previous work on sunfish dorsal fins (Drucker and Lauder, 2001a). Steady rectilinear locomotion in trout was elicited at three speeds: 0.5, 1.0 and 2.0 L s^{-1} (range, 9–42 cm s^{-1}). In addition, fish performed yawing turns in response to a visual and auditory stimulus as in previous work on sunfish (Drucker and Lauder, 2001b). While trout swam steadily at 0.5 L s^{-1}, a small-diameter wooden dowel was directed into the water approximately 20 cm lateral to the head to induce yawing maneuvers. The fish's immediate response to this stimulus and the lateral location of the dowel precluded any interaction between the dorsal fin wake and the wake shed by the dowel. To characterize patterns of movement of the dorsal fin during both steady swimming and maneuvering, fish were imaged simultaneously in lateral and dorsal aspect using synchronized digital high-speed video cameras (Redlake MotionScope PCI 500; San Diego, CA, USA) operating at 250 frames s^{-1} (1/250 s shutter speed). Review of these light video recordings revealed general patterns of activity- and speed-dependence of fin kinematics.

In separate swimming trials, the wake of the dorsal fin was visualized using digital particle image velocimetry (DPIV). We employed this technique to obtain empirical, quantitative information about momentum flow in two-dimensional sections of the fluid moved by the fish's propulsors (as described in detail by Drucker and Lauder, 1999, 2001b; Lauder, 2000; Willert and Gharib, 1991). An 8 W continuous-wave argon-ion laser (Coherent Inc., Santa Clara, CA, USA) was focused into a thin light sheet (1–2 mm thick, 16 cm wide) that illuminated reflective microparticles suspended in the water. Particle motion induced by fin activity was recorded by imaging the laser sheet with one of the Redlake video cameras (250 frames s^{-1}, 1/1000 s shutter speed). Wake flow was observed in the frontal (horizontal) plane from a dorsal perspective by means of a mirror inclined at 45° above the working area. A second camera synchronously recorded a perpendicular (lateral) reference view, showing the position of the fish and its fins relative to the visualized transection of the wake. The horizontal laser plane was positioned at three heights along the dorsoventral body axis of the fish (Fig. 1A). This variable positioning of the laser plane allowed measurement of the structure and strength of vortices shed by the soft dorsal fin alone during steady swimming and turning (Fig. 1A, plane 1) and observation of the tail's interaction with the dorsal fin's wake (Fig. 1A, plane 2). Trout occasionally swam with the adipose fin also within the light sheet at plane 2, providing a simultaneous view of all three dorsal median fins. In its lowest position (Fig. 1A, plane 3), the laser plane intersected the tail at mid-fork. Flow patterns within this plane were used to characterize the structure of the tail's wake and to estimate caudal-fin swimming forces, which provided a context for interpreting calculated dorsal fin forces.

Kinematic and hydrodynamic measurements

To quantify temporal and spatial patterns of median fin motion during steady swimming, selected video frames were analyzed using ImageJ software. For each of three fish, we measured the mediolateral excursions of all median fins visible in dorsal aspect within the horizontal laser plane (Fig. 1A, plane 2). Specifically, over the course of five consecutive fin beats performed at each swimming speed, we tracked the position of the trailing edges of the dorsal and adipose fins, and the position of the leading edge of the caudal fin, in alternate video frames (i.e. at 8 ms intervals). Tracking movement of the leading edge of the caudal fin, as opposed to the trailing edge, enabled assessment of potential hydrodynamic interactions between the anterior portion of the tail and the dorsal fin wake produced upstream. Body reference points (pigment spots) at longitudinal positions corresponding to the tips of the dorsal and adipose fins were also digitized. These data collectively allowed (1) graphical representation of fin-tip trajectories in excursion–time plots, with each fin beat cycle comprised of approximately 30–50 points; (2) analysis of the speed dependence of kinematic parameters such as fin beat frequency and mediolateral fin sweep amplitude; (3) measurement of the phase lag of oscillatory motion between more anteriorly and posteriorly situated median fins; and (4) calculation of the Strouhal number, the product of fin beat frequency and peak-to-peak sweep amplitude divided by swimming speed, which serves as a theoretical predictor of propulsive efficiency (Anderson et al., 1998; Triantafyllou et al., 1993).

From DPIV video sequences, 130 swimming events performed by six fish were reviewed to establish general patterns of water flow in the wake. Of these, detailed quantitative analysis was restricted to scenes in which fish swam at a constant speed either during prolonged rectilinear locomotion (N=9–33 fin beats per behavior) or immediately before turning maneuvers (N=14). For the purpose of calculating stroke-averaged locomotor force, the duration of

propulsive fin movement, τ, was measured from each swimming sequence. For steady swimming, τ was defined as the stroke period of median fin oscillation (i.e. the interval in ms separating the position of maximal left or right excursion of the fin tip and the analogous position in the immediately following stride). For turning, during which vortical wake structures were generated over the course of a single half-stroke, τ was taken as the duration of dorsal fin abduction and following adduction to the midline.

Two-dimensional water velocity fields in the wake of trout were calculated from consecutive digital video images (480 pixels×420 pixels, 8-bit grayscale) by means of spatial cross-correlation (Willert and Gharib, 1991), as in our previous research (e.g. Drucker and Lauder, 1999, 2000, 2001b; Lauder and Drucker, 2002). The relatively weak wake flows generated by the trout dorsal fin were resolved using a recursive local-correlation image-processing algorithm (Hart, 1998) implemented by InsightUltra software (TSI Inc., St Paul, MN, USA; also see Lauder et al., 2002). We measured frontal-plane flow fields that were 7–10 cm on each side and comprised nearly 2300 uniformly distributed velocity vectors (i.e. 52 horizontal × 44 vertical, or 30 vectors cm^{-2}). Vectors falling within regions of shadow cast by the fish, or overlying the body within laser planes close to the illuminated skin surface (e.g. Fig. 1A, plane 2), were misrepresentative of actual water flow and were deleted manually from flow fields. For all swimming behaviors, the mean free-stream flow velocity of the flume was subtracted from each vector matrix to reveal vortical structures in the wake and to allow measurement of jet flow structure and strength (for details, see Drucker and Lauder, 1999). Vortex circulation was calculated using a custom-designed computer program. Jet flow velocity was taken as the mean magnitude of vectors (N=247 on average) comprising the central region of accelerated flow within the frontal plane. For both steady swimming and turning, jet angle was defined as the mean orientation of these vectors, measured relative to the upstream heading of the fish at the onset of the fin stroke. Both jet measurements were made at the end of median fin adduction, at which time vortices and associated jet flow were fully developed.

In previous DPIV studies of fish locomotion, we have examined wake flow in multiple, perpendicular orientations of the laser light sheet (e.g. Drucker and Lauder, 1999, 2000), allowing three-dimensional reconstruction of wake geometry. In the present study, visualization of the wake was restricted to the horizontal plane; vertically oriented laser sheets (i.e. in the parasagittal and transverse planes) projected from below are obstructed by the body of the fish itself and were therefore not employed. However, earlier DPIV work examining flow within orthogonally oriented laser planes supports a three-dimensional vortex-ring wake structure for the median fins of fishes (Lauder, 2000; Liao and Lauder, 2000; Nauen and Lauder, 2002a; Wolfgang et al., 1999). On this basis, we used flow measurements from frontal-plane transections of the dorsal and caudal fin wakes to estimate vortex-ring morphology and associated fluid forces generated during locomotion. We assumed that paired vortices observed in the frontal plane represent approximately mid-line sections of a toroidal vortex ring. Ring momentum was calculated as the product of water density, mean vortex circulation and ring area (the latter two measurements made at the end of the fin stroke). Ring area was taken as πR^2, where R is half the distance between paired vortex centers. Following earlier work (Milne-Thomson, 1966), time-averaged wake force was then computed as the momentum added to the wake divided by the period of propulsive fin motion. Total force exerted by each median fin was resolved geometrically into perpendicular components within the frontal plane (thrust and lateral force) according to the mean jet angle. Further details of the calculation of wake force magnitude and orientation by this method can be found in earlier studies (Dickinson, 1996; Dickinson and Götz, 1996; Drucker and Lauder, 1999, 2001a, 2003; Lauder and Drucker, 2002; Spedding et al., 1984).

Results

Behavioral and kinematic patterns

Rainbow trout recruit the dorsal fin both during steady swimming over a range of speeds and during unsteady turning maneuvers. While swimming straight ahead, trout erect the dorsal fin at low speeds and gradually depress the fin as speed increases (Fig. 2A,C). The extent to which the dorsal fin is erected from the body at each speed shows interindividual variation (e.g. compare Fig. 2A in this paper with fig. 1A in Drucker and Lauder, 2003), but the general negative speed dependence of dorsal fin height was consistently observed. Additionally, trout oscillate the trailing edge of the dorsal fin from side to side during constant-speed, rectilinear locomotion. At low speed (0.5 $L\ s^{-1}$), the amplitude of dorsal fin oscillation markedly exceeds that of the body at the same longitudinal position (Fig. 3A). As swimming speed increases (1.0 $L\ s^{-1}$), dorsal fin amplitude decreases while body amplitude increases (Fig. 3C), until at the highest speed studied (2.0 $L\ s^{-1}$) the dorsal fin and body undergo nearly identical side-to-side excursions over the course of the stroke cycle (Fig. 3E). To separate motion of the dorsal fin from that of the underlying body, we corrected dorsal fin beat amplitudes at each speed by calculating the difference between the maximal side-to-side excursion of the dorsal fin's trailing edge (i.e. the uncorrected amplitude) and the sweep amplitude of the corresponding body reference point. The magnitude of side-to-side oscillation of the dorsal fin, beyond that of the body, drops by a factor of two between 0.5 and 1.0 $L\ s^{-1}$ and approaches zero at 2.0 $L\ s^{-1}$ (Table 1).

In contrast to the dorsal fin, the adipose fin of trout exhibits negligible motion independent of the body during steady swimming. Adipose fin height does not change measurably during slow and fast locomotion, and although adipose fin-beat frequency and peak-to-peak fin beat amplitude increase with speed (Fig. 3B,D,F), these kinematic parameters are not significantly different from those of the body at the same longitudinal position (paired t-tests at 0.5, 1.0 and 2.0 $L\ s^{-1}$; d.f.=4; P=0.2–1.0). Corrected adipose stroke amplitude remains near zero (<0.1 cm) at all swimming speeds examined (Table 1).

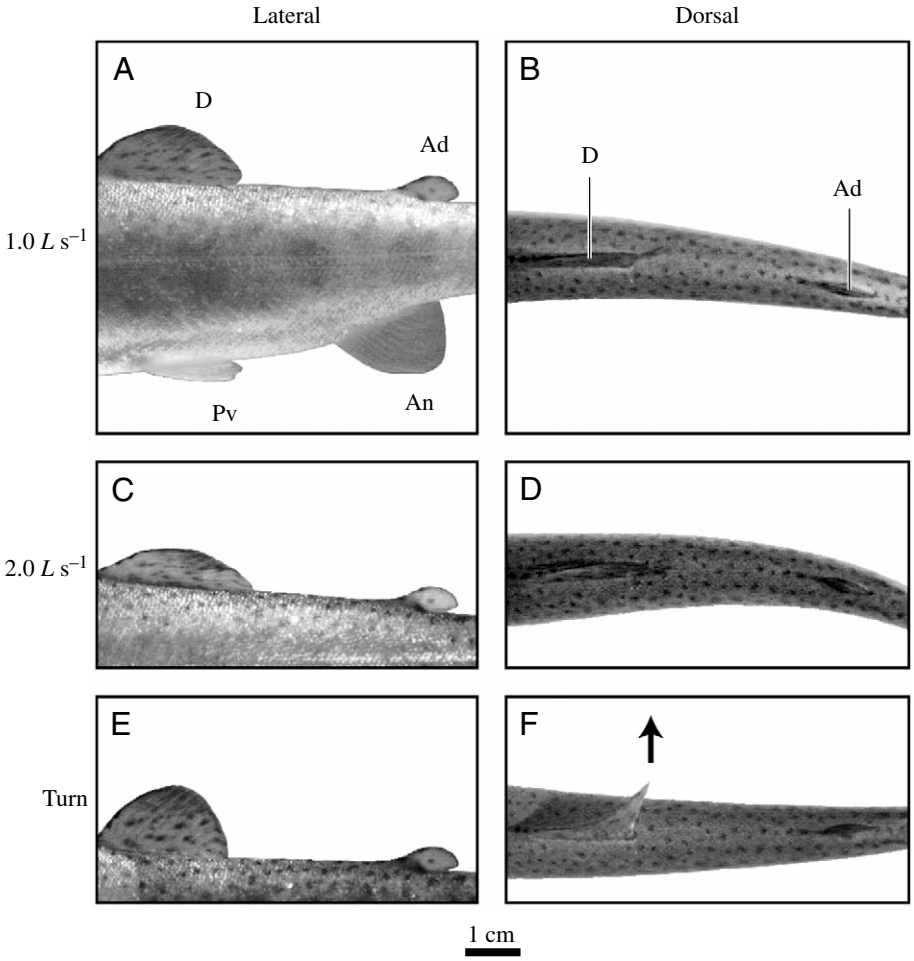

Fig. 2. Light video images of the posterior trunk and fins of rainbow trout during steady swimming at two speeds and during turning. Lateral and dorsal image pairs for each behavior were recorded simultaneously. As swimming speed increases from 1.0 to 2.0 body lengths (*L*) s^{-1}, dorsal fin height decreases, while the height of the adipose fin remains unchanged (A,C). During turning, the dorsal fin is erected (E) and moves unilaterally (indicated by arrow in F) toward the stimulus, causing body rotation in the opposite direction. Ad, adipose fin; An, anal fin; D, soft dorsal fin; Pv, pelvic fin.

Mean trailing-edge amplitude of the caudal fin (uncorrected) measured from 0.5–2.0 *L* s^{-1} exceeds that of the dorsal and adipose fins anteriorly by 0.29–2.15 and 1.34–1.81 cm, respectively. For all three dorsal median fins, the frequency of mediolateral oscillation shows a direct dependence on swimming speed, and at each speed this frequency shows no significant difference among fins (two-way analysis of variance; speed effect, $F_{2,72}$=202.89; P<0.001; fin effect, $F_{2,72}$=0.45; P=0.64; also see Fig. 3; Table 1).

Unlike steady swimming, low-speed turning maneuvers elicited from trout are characterized by non-periodic dorsal fin activity. At the onset of a turn, trout erect the dorsal fin and unilaterally abduct it to the side of the body towards which the experimental stimulus is directed (Fig. 2E,F). This fin motion is accompanied by ipsilateral abduction of the pectoral and pelvic fins (also see fig. 3 in Drucker and Lauder, 2003). Relatively rapid fin adduction follows; for the dorsal fin, the total duration of propulsive fin motion is considerably less than that during steady swimming (Table 2). Together with low-amplitude bending of the trunk, these median and paired fin motions cause both yawing rotation (mean, 13 deg. s^{-1}; Drucker and Lauder, 2003) and translation of the body away from the source of the stimulus.

Wake dynamics

The structure and strength of the wake produced by the dorsal fin of trout vary markedly with swimming behavior. During steady, straight-ahead locomotion at low speed (0.5 *L* s^{-1}), each

Table 1. *Speed effects on median fin kinematics in rainbow trout*

Swimming speed (L s^{-1})	Dorsal fin		Adipose fin		Caudal fin	
	f (Hz)	a (cm)	f (Hz)	a (cm)	f (Hz)	a (cm)
0.5	2.49±0.09	1.51±0.03 (1.23±0.06)	2.40±0.03	0.46±0.04 (0.04±0.01)	2.48±0.02	1.80±0.14
1.0	3.15±0.06	1.21±0.08 (0.56±0.07)	3.21±0.06	0.74±0.02 (0.05±0.01)	3.18±0.05	2.55±0.14
2.0	4.15±0.17	0.70±0.05 (0.03±0.01)	4.17±0.08	1.13±0.03 (0.01±0.01)	4.23±0.16	2.85±0.04

Values are means ± S.E.M. (N=5 stroke cycles from each of three fish per measurement).

f, fin beat frequency; a, fin beat amplitude (maximal side-to-side excursion of trailing edge). For the dorsal and adipose fins whose mediolateral excursions are influenced by body undulation, a corrected measure of a is reported in parentheses in addition to absolute a. Corrected amplitude is calculated as the mean difference between absolute fin sweep amplitude and body bending amplitude (cf. Fig. 3). For the caudal fin, a is the absolute sweep amplitude.

L, total body length (mean 19.6 cm).

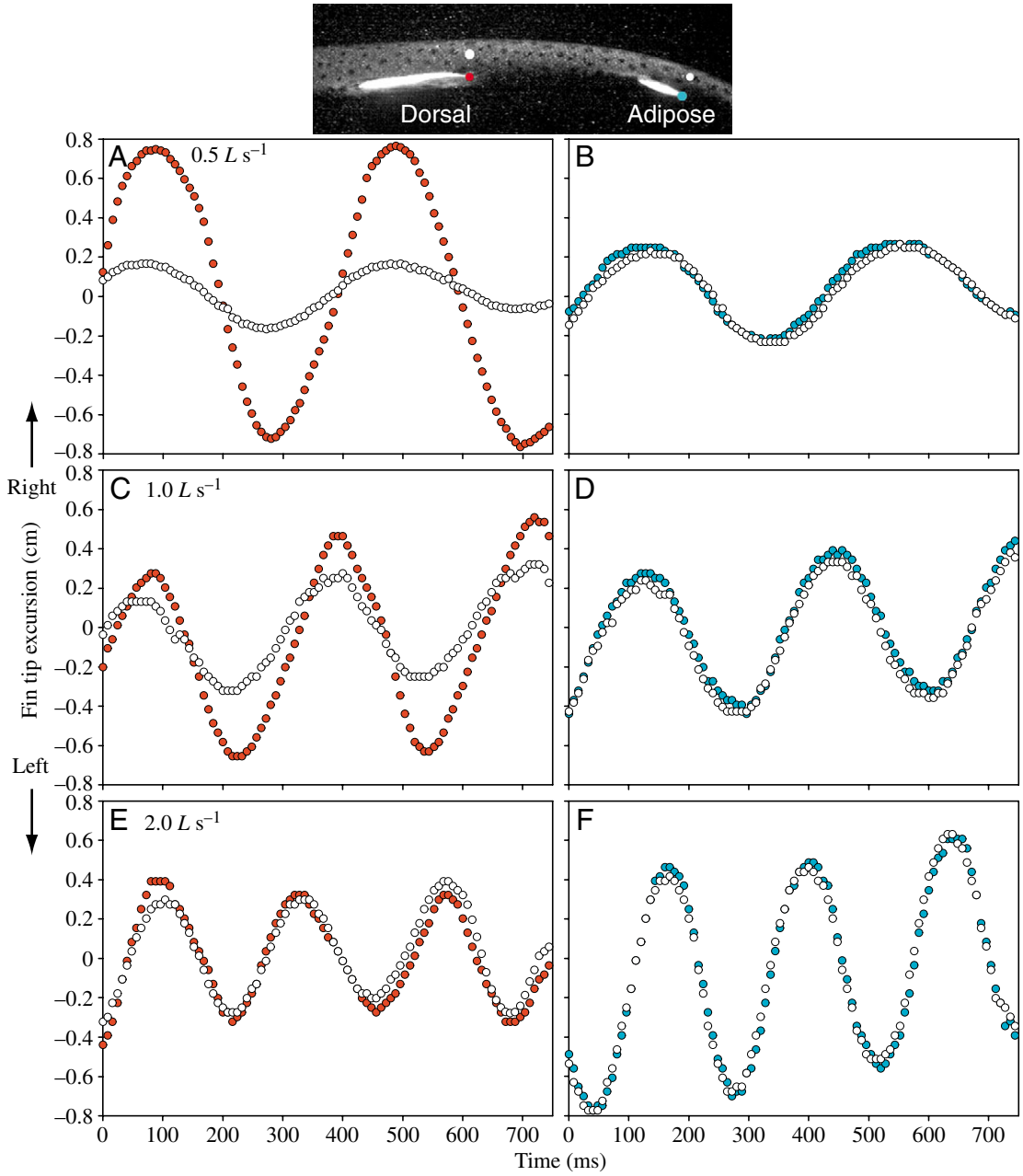

Fig. 3. Kinematic patterns for the soft dorsal and adipose fins of trout oscillating in tandem during steady swimming at three speeds. The image at the top illustrates the points digitized from dorsal-view video (Fig. 1A, plane 2): red and blue symbols indicate the trailing edges of the dorsal and adipose fins, respectively, with body reference points at corresponding longitudinal positions represented by white symbols. At low swimming speed (0.5 L s^{-1}), the amplitude of dorsal fin oscillation exceeds the amplitude of body bending (A), while the excursion of the adipose fin closely tracks that of the body (B). With increasing speed (1–2 L s^{-1}) dorsal fin amplitude declines as body amplitude increases (C) until the dorsal fin's trailing edge and the body exhibit nearly identical excursion patterns (E). At higher speeds, the frequency and amplitude of adipose fin oscillation continue to match those of the body (D,F).

complete stroke of the dorsal fin generates a distinct wake visible within the frontal plane as paired counter-rotating vortices with interposed jet flow (e.g. structure 2 in Fig. 4). The development of this wake morphology involves (1) excursion of the dorsal fin from a maximally abducted position to a corresponding contralateral position, which entrains jet flow from one side of the body to the other (structure 3, Fig. 4A) and generates a free vortex at the downstream edge of the jet (partially obscured by body reflection in Fig. 4A; cf. Drucker and Lauder, 2001a); (2) rapid stroke reversal and return of the fin to its original position, during which a second free vortex of opposite-sign rotation is shed and the jet is strengthened (structure 3, Fig. 4B). This subsequent fin motion additionally initiates the jet flow of the next half-stroke (structure 4, Fig. 4B). During continuous dorsal fin oscillation at 0.5 L s^{-1},

Table 2. *Hydromechanical measurements from dorsal- and caudal-fin swimming behaviors by rainbow trout*

	Dorsal fin			Caudal fin
Measurement	Steady swimming at 0.5 L s^{-1}	Steady swimming at 1.0 L s^{-1}	Turning	Steady swimming at 1.0 L s^{-1}
Duration of propulsive fin movement (ms)	406±14.6	320±5.5	144±4.5	314±7.2
Mean jet angle (deg.)	75.5±2.7	75.4±4.7	87.8±3.0	69.8±1.6
Mean jet velocity (cm s^{-1})	3.9±0.2	4.0±0.2	4.0±0.3	5.2±0.1
Force, lateral component				
Absolute (mN)	0.62±0.16	2.20±0.51	1.79±0.46	13.62±0.61
Corrected (mN cm^{-2})	0.10±0.03	0.36±0.08	0.30±0.08	–
Force, posterior component				
Absolute (mN)	0.16±0.05	0.42±0.09	0.11±0.05	5.47±0.62
Corrected (mN cm^{-2})	0.03±0.01	0.07±0.02	0.02±0.01	–
Force ratio, lateral:posterior	5.2±1.2	5.8±1.4	14.0±3.8	4.0±0.8
Strouhal number	0.375±0.001	0.206±0.015	–	0.382±0.011

Values are means ± S.E.M. (N=6 fish). Dorsal fin measurements are reported for steady swimming at 0.5 and 1.0 L s^{-1} (N=9 and 25 events, respectively) and for turning immediately following steady swimming at 0.5 L s^{-1} (N=14). Caudal fin data are for steady swimming at 1.0 L s^{-1} (N=33). Mean total body length, L=19.6 cm.

Wake measurements were made from frontal-plane velocity fields (see Fig. 1A). Jet angles less than 90° indicate wake jets oriented downstream. Jet velocities are measures taken above the mean free-stream flow velocity. Lateral and posterior (thrust) forces are averages over the stroke duration (i.e. associated with a single vortex pair) calculated as wake momentum divided by the duration of propulsive fin movement. Corrected force is expressed as absolute dorsal fin force divided by dorsal fin area.

multiple vortex pairs persist within the horizontal laser plane, with their associated fluid jets alternating to the left and right sides of the body. Over time, these structures migrate laterally, pass through the laser plane and ultimately lose their paired-vortex appearance (structure 1, Fig. 4).

During steady swimming at higher speed (1.0 L s^{-1}), the dorsal fin continues to shed a wake comprised of both vortical and linear (i.e. jet) flows (Fig. 5). The mean velocity and orientation of the wake jet do not change significantly between 0.5 and 1.0 L s^{-1} (unpaired t-tests; d.f.=21; P=0.70 and 0.99, respectively; Table 2). However, the dorsal fin stroke is performed more rapidly at 1.0 L s^{-1} (mean difference in stroke duration, 86 ms), leading to a marked increase in fluid force production (Table 2). In addition, there is a notable difference in the geometry of the wake generated during slow and fast swimming. At 1.0 L s^{-1}, the vortex shed at the end of each half-stroke coalesces with the same-sign vortex produced at the onset of the next half-stroke (forming a 'stopping–starting' vortex; cf. Drucker and Lauder, 2001a). The wake at this speed is therefore comprised of a continuous, nearly linear trail of counter-rotating vortices aligned with the body axis (Fig. 5), as opposed to discrete vortex pairs on opposite sides of the body (cf. Fig. 4). Trout wake flow patterns at 0.5 and 1.0 L s^{-1} are schematically summarized and compared in Fig. 8A,B.

At the highest speed studied (2.0 L s^{-1}), the dorsal fin is no longer recruited to add momentum to the wake (Fig. 6). Moving with the same frequency and amplitude as the body (Fig. 3E), the trailing edge of the dorsal fin contributes to small-scale turbulence along the dorsal midline of the body but does not generate propulsive fluid jets (Fig. 6) as at lower speeds.

Turning maneuvers, by contrast, are characterized by relatively strong rotational wake flows and associated fluid jets on one side of the body. Low-speed yawing rotation of the body involves the production of a pair of counter-rotating vortices during a single half-stroke of the dorsal fin (Figs 7, 8C). The mean velocity of the turning jet is not significantly different from that measured during steady swimming at 0.5 or 1.0 L s^{-1} (unpaired t-tests; d.f.=17, 22; P=0.72, 0.97, respectively). This jet, however, is oriented at nearly 90° to the initial heading of the fish before the turn (i.e. directed 12° further laterally, on average, than during steady swimming). Accordingly, the ratio of laterally to posteriorly oriented wake force during turning is relatively large (Table 2).

Of the three dorsally situated median fins, the adipose fin alone sheds a poorly organized drag wake (cf. Drucker and Lauder, 2002a) during all swimming behaviors studied. At a gross level, this small fin (mean area ± S.D.=0.59±0.12 cm^2, N=4 fish) generates no propulsive momentum flows. By contrast, the caudal fin of trout sheds a trailing wake similar to that produced by the caudal fin of other fishes swimming by subcarangiform locomotion. The tail wake of trout, illustrated in fig. 3 of Lauder et al. (2002), resembles the continuous vortex trail shed by the dorsal fin at 1.0 L s^{-1} (Fig. 5). The caudal fin generates a wake jet with an orientation comparable to that of the dorsal fin (mean jet angle, 70–75°), such that the ratio of lateral-to-posterior (thrust) force for both fins falls within the range of 4–6 during steady swimming (Table 2). Mean lateral and thrust forces produced by the dorsal fin at 1.0 L s^{-1} represent 16% and 8%, respectively, of the corresponding tail forces. When corrected for interindividual variation in dorsal fin area (mean ± S.D.=6.03±0.70 cm^2) dorsal fin forces ranged from approximately 0.02 to 0.36 mN cm^{-2} for all behaviors studied in rainbow trout (Table 2).

Lateral oscillations of the trailing edge of the dorsal fin and

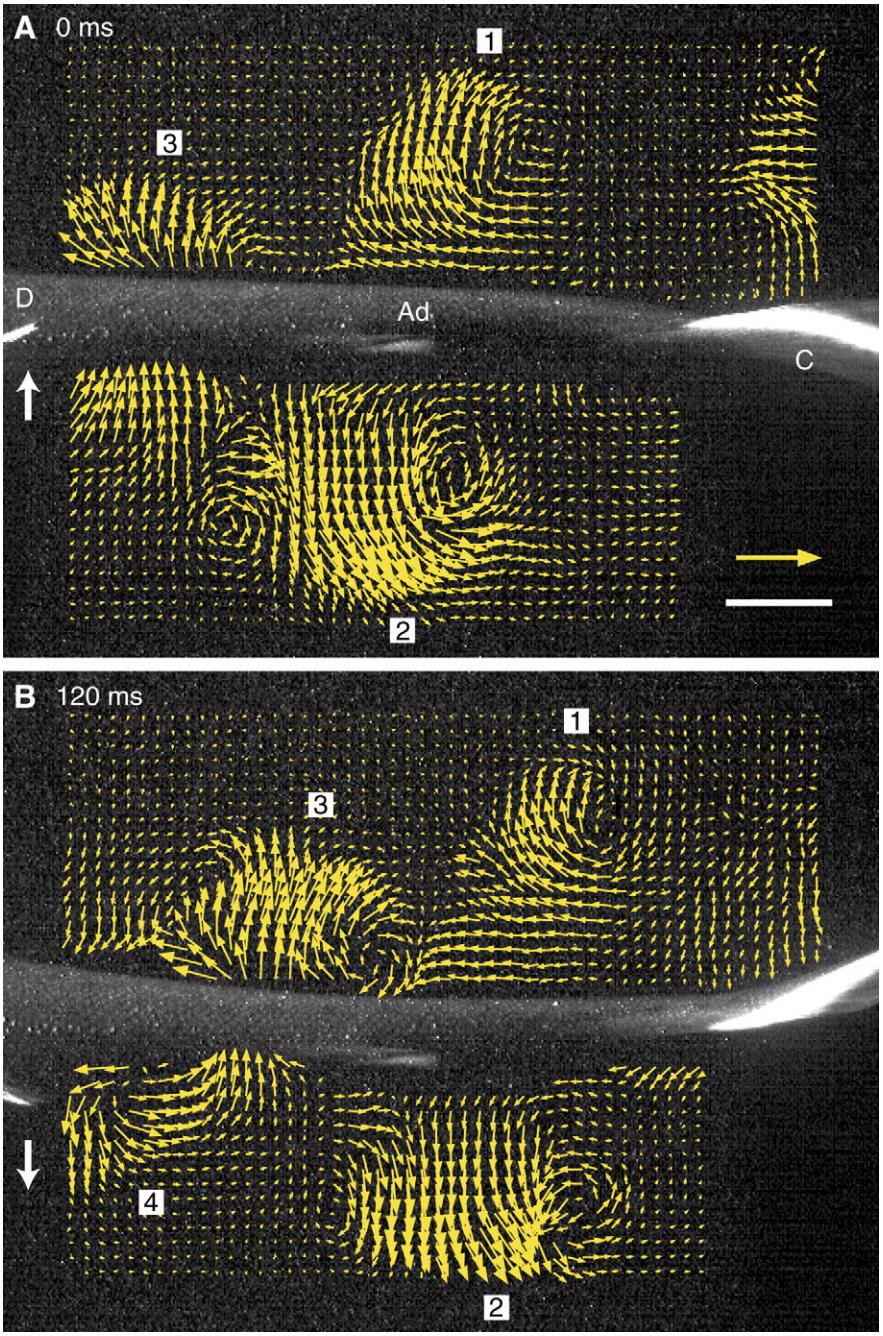

Fig. 4. Visualization of the dorsal fin wake during steady swimming at 0.5 L s^{-1} by rainbow trout. The frontal-plane wake velocity field (Fig. 1A, plane 2) is shown as a matrix of yellow vectors on either side of the body; vectors overlying the body have been deleted. The trailing edge of the dorsal fin (D) is visible at the left of each panel, with white arrows indicating the direction of its movement. The adipose fin (Ad) and caudal fin (C) are also illuminated by the light sheet. Flow fields are shown at two times corresponding to the end of dorsal fin movement to the right (A) and the end of the next half-beat to the left (B). Vortical wake structures generated by the dorsal fin are numbered 1–4 in order of their appearance within the frontal plane. Structure 1 is the oldest, having been generated by the dorsal fin stroke to the right preceding that illustrated in A. The paired vortex morphology characteristic of younger wake elements is no longer evident in structure 1. Structure 2, formed during the stroke to the left preceding that shown in B, is a well-developed vortex pair with central jet flow. Structure 3, formed by the fin motions shown in A and B, has the same morphology as structure 2 but is situated on the opposite side of the body. Structure 4 is the youngest wake element, part of an incipient vortex pair and produced by the dorsal fin stroke to the left illustrated in B. Note that the dorsal fin wake at this low swimming speed is comprised of vortex centers located on each side of the body and that wake jets are oriented posterolaterally. Free-stream velocity of 8.5 cm s^{-1} has been subtracted from the vector fields to highlight vortices. Yellow scale arrow, 10 cm s^{-1}; white scale bar, 1 cm.

the leading edge of the caudal fin are approximately one-quarter cycle out of phase with each other during steady rectilinear locomotion at 1.0 L s^{-1} (phase lag=99±4 ms, 114±3°, means ± S.E.M.; Fig. 9A–E). As a result, the leading edge of the caudal fin traces a path directly through the centers of the vortices shed by the dorsal fin and passes through the developing lateral jet flows formed between vortex centers (Fig. 9F).

Discussion

Dorsal fin recruitment and effects of swimming speed

Use of the dorsal fin by salmoniform fishes as an ancillary thrust generator during steady axial locomotion has not previously been documented either by field observation (e.g. McLaughlin and Noakes, 1998) or laboratory study (Webb, 1971, 1991; Webb et al., 1984). The present study identifies two important patterns of dorsal fin recruitment in trout during rectilinear swimming. First, involvement of the dorsal fin in locomotor dynamics *decreases* with increasing swimming speed. When hovering (0 L s^{-1}) and swimming forward at low speed (0.5 L s^{-1}), trout fully erect the dorsal fin and exhibit the largest mediolateral dorsal fin excursions (Fig. 3; Table 1). Accordingly, the dorsal fin is expected to accelerate the largest volumes of water during these slow swimming behaviors. With increasing speed (1–2 L s^{-1}), both dorsal fin height and sweep amplitude decline sharply (Figs 2, 3; Table 1). This

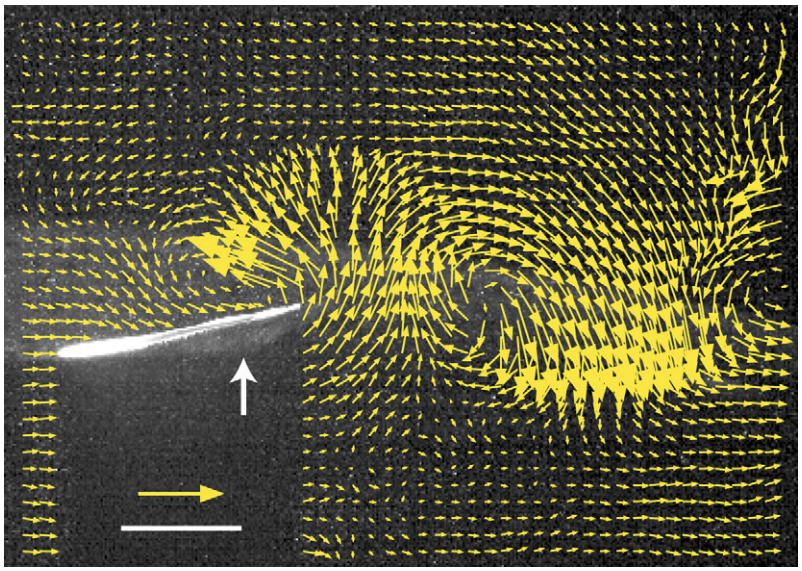

Fig. 5. Visualization of the dorsal fin wake during steady swimming at 1.0 L s^{-1} by rainbow trout. The frontal-plane light sheet is at position 1 (Fig. 1A), intersecting the middle of the dorsal fin, which is erected at this speed (see Fig. 2A); all other conventions follow those of Fig. 4. Note the continuous trail of vortex centers over the body, a wake morphology that stands in contrast to the discrete, bilaterally positioned vortex pairs observed at 0.5 L s^{-1} (Fig. 4). Free-stream velocity of 19.4 cm s^{-1} has been subtracted from the vector field. The white arrow shows the direction of dorsal fin movement. Yellow scale arrow, 10 cm s^{-1}; white scale bar, 1 cm.

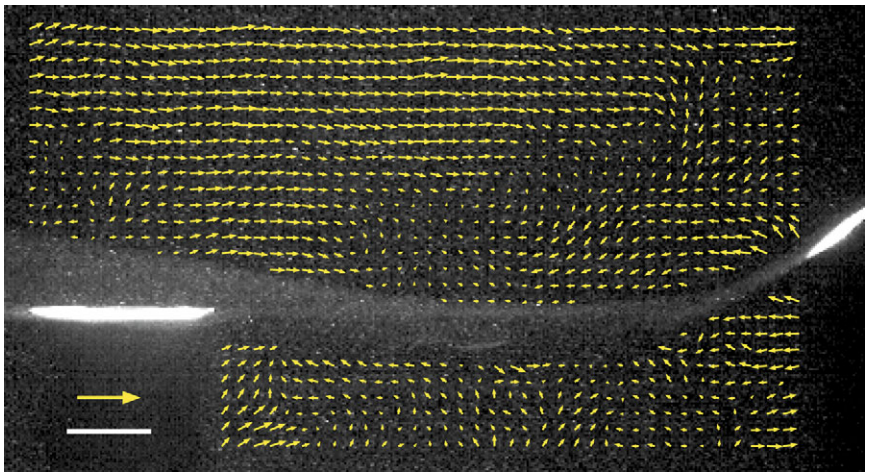

Fig. 6. Visualization of the dorsal fin wake during steady swimming at 2.0 L s^{-1} by rainbow trout. The frontal-plane light sheet is at position 2 (Fig. 1A), intersecting the middle of the dorsal fin (at left), which is depressed at this speed (see Fig. 2C). The caudal fin is visible at the far right; all other conventions follow those of Fig. 4. Note the absence of vortex centers and fluid jets; background turbulence dominates the dorsal fin wake at this speed. This wake morphology contrasts sharply with the strong dorsal fin vortices and propulsive jets observed at lower swimming speeds (Figs 4, 5). Free-stream velocity of 38.4 cm s^{-1} has been subtracted from the vector field. Yellow scale arrow, 10 cm s^{-1}; white scale bar, 1 cm.

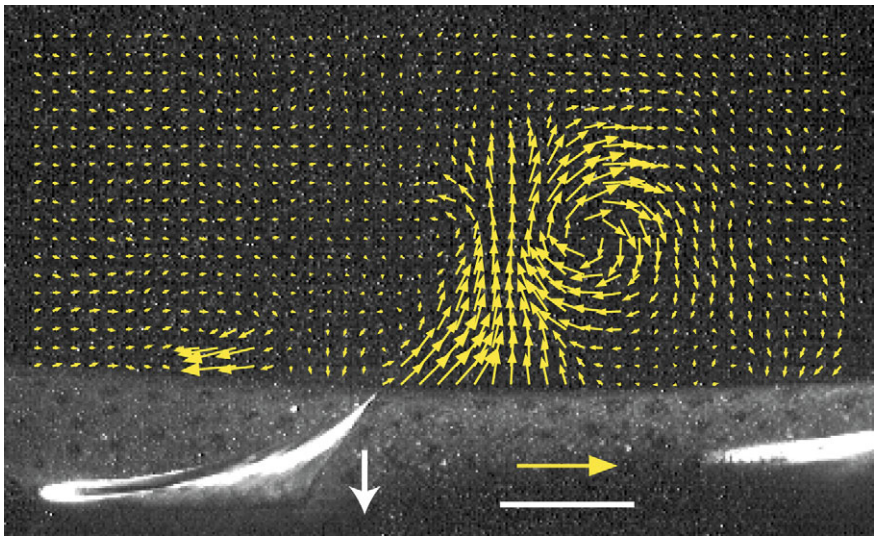

Fig. 7. Visualization of the dorsal fin wake during a slow turn at 0.5 L s^{-1} by rainbow trout. The frontal-plane light sheet is at position 2 (Fig. 1A), and vectors overlying the body have been deleted; the dorsal fin is visible to the left and the adipose fin to the right. This image shows the dorsal fin soon after it has reached maximal excursion to the right of the body and has begun the return stroke toward the midline (indicated by the white arrow pointing to the left of the body). Unilateral dorsal fin abduction results in the well-developed vortex with clockwise rotation and the strong laterally directed jet. During the return stroke, the counterclockwise member of the vortex pair develops, the wake jet is strengthened and the fish's body yaws to the left. Free-stream velocity of 8.5 cm s^{-1} has been subtracted from the vector field. Yellow scale arrow, 10 cm s^{-1}; white scale bar, 1 cm.

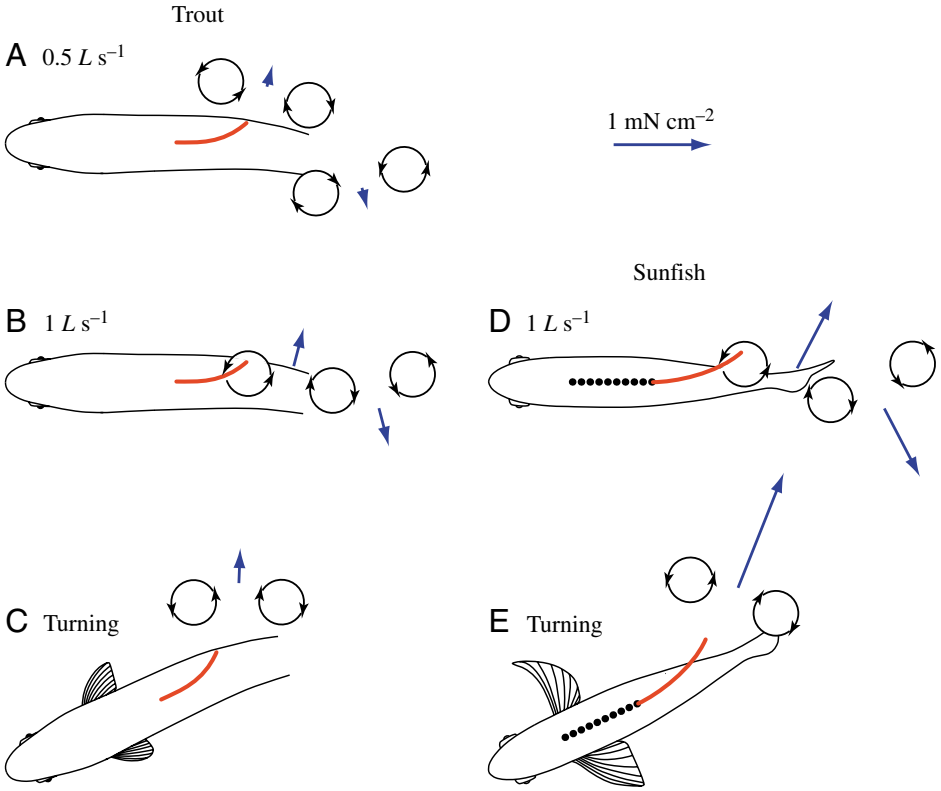

Fig. 8. Schematic summary of dorsal-fin vortex wake patterns observed in rainbow trout during steady swimming (A,B) and turning (C), compared with previously described patterns in bluegill sunfish performing similar steady swimming and turning behaviors (D,E) (sunfish data from Drucker and Lauder, 2001a). Turning behavior in both species was initiated during steady swimming at 0.5 L s^{-1}. Line drawings of the fishes are not precisely to scale (although individuals of both species were approximately 20 cm in total length). The soft dorsal fin is shown in red and the cores of associated wake vortices are represented by curved arrows (note that the counterclockwise vortex in C was not consistently well developed within the horizontal laser plane). Blue vectors indicate both the mean orientation and magnitude of stroke-averaged force within the horizontal plane (normalized to soft dorsal fin area). In general, trout generate dorsal fin forces of lower relative magnitude and with more lateral orientation than sunfish during comparable swimming behaviors.

recruitment pattern stands in contrast to that observed for other dorsal fin swimmers studied thus far. Unlike the short-based, oscillatory dorsal fin of trout, representative of the basal teleost condition, the more elongate, undulatory dorsal fin of balistid fishes (members of the derived Acanthomorpha) is actively employed over a wide range of swimming speeds (up to approximately 4–8 L s^{-1}; Korsmeyer et al., 2002; Wright, 2000). Similarly, the soft dorsal fin of sunfish (*Lepomis*) is hydrodynamically inactive at low speed (0.5 L s^{-1}) and generates a propulsive vortex wake at higher speed (1.0 L s^{-1}) (Drucker and Lauder, 2001a).

A second notable pattern in dorsal fin recruitment by trout is evident in the gait transition that occurs between low- and higher-speed swimming. The range of locomotor behaviors exhibited by aquatic vertebrates can be partitioned into functional categories according to the anatomy and kinematics of the propulsors involved. Webb (1984) proposed several such categories for fishes including 'median and paired fin' (MPF) propulsion and 'body and caudal fin' (BCF) locomotion. The idealized gait progression expressed with increasing swimming speed is MPF→BCF (Webb, 1994, p. 11; Webb and Gerstner, 2000). This influential scheme has inspired much research on swimmers at the extremes of the gait continuum, but only relatively recently has close attention been given to swimming modes involving a combination of the MPF and BCF gaits.

In this paper, we document, in trout swimming steadily at low to intermediate speeds, the combined use of dorsal fin oscillation and axial undulation (Figs 3A,C, 9F) without continuous concomitant pectoral fin motion. Simultaneous recruitment of anterior median fin propulsion together with body and caudal fin locomotion define an aquatic gait we term M–BCF. A similar fin-use pattern has been observed for balistiform swimmers at high speed (Korsmeyer et al., 2002; Wright, 2000). This gait is distinct from the MPF–BCF swimming mode described for certain ostariophysan fishes, in which pectoral, dorsal and anal fin beating occurs together with 'small-amplitude' caudal fin undulation during forward swimming (Webb and Gardiner Fairchild, 2001). For trout, the range of steady swimming speeds over which the pectoral fins are recruited is compressed (0–0.5 L s^{-1}), such that MPF locomotion is restricted largely to hovering in still water (Drucker and Lauder, 2003), and forward swimming is characterized by the gait transition from M–BCF to BCF propulsion (which occurs just below 2.0 L s^{-1} for fish 20 cm in length). Detailed study of paired and median fin motion in other clades lacking specialized swimming modes will contribute further to our understanding of the diversity of locomotor behaviors employed by teleost fishes.

The observation of periodic dorsal fin oscillation in trout raises an important functional question: does the fin move actively and independently from the body to which it is attached? The soft dorsal fin of teleost fishes is invested with segmentally arranged muscles, distinct from the myomeric muscle mass, that are capable of controlling mediolateral motion of the propulsive fin surface. On both sides of the body, dorsal inclinator muscles arise from the fascia overlying the epaxial myomeres and insert onto the lateral base of each flexible dorsal fin ray, thereby enabling fin abduction (Geerlink

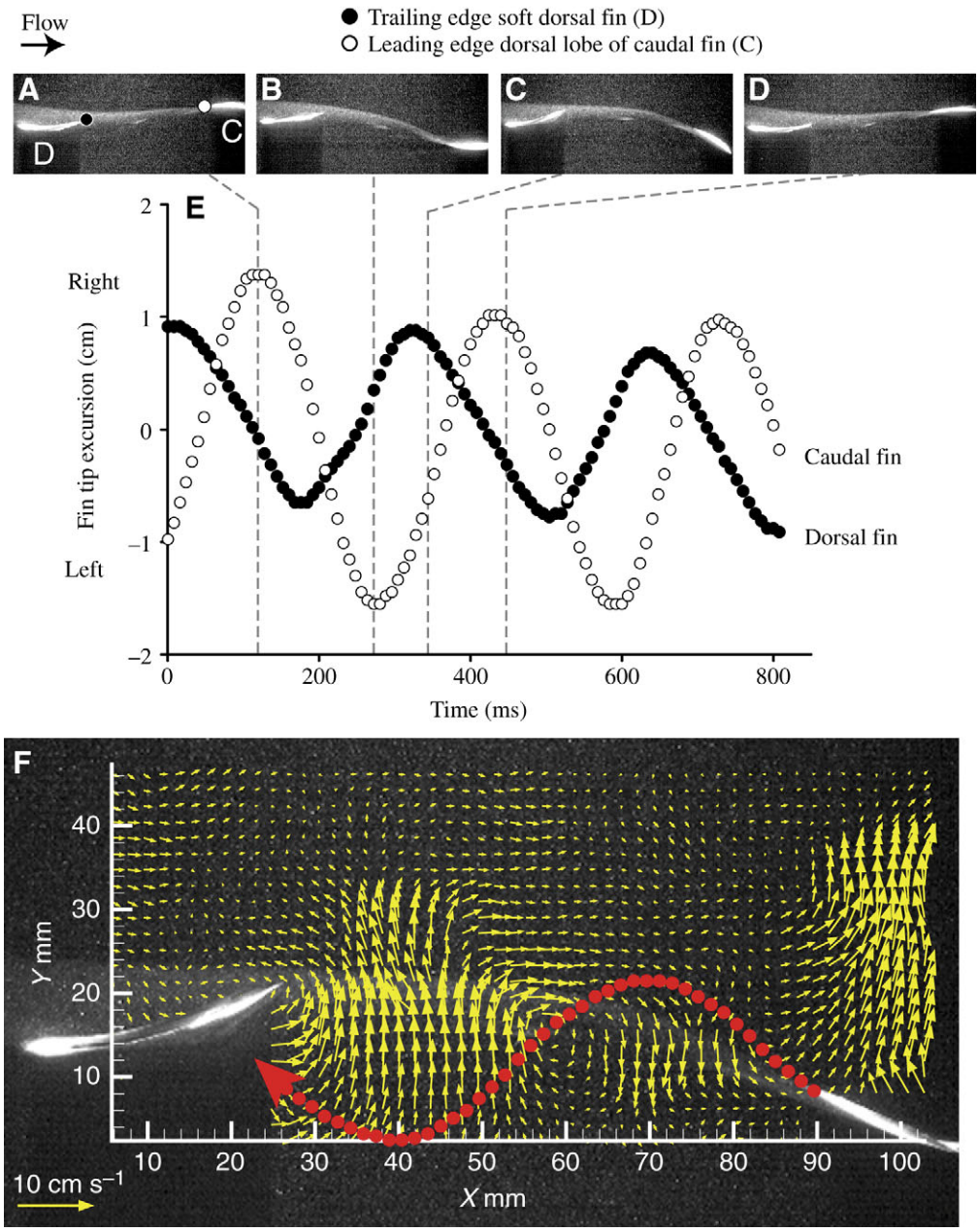

Fig. 9. Dorsal–caudal fin kinematic phase relationship and hydrodynamic interaction in rainbow trout. (A–D) Dorsal-view video frames showing mediolateral excursion of the trailing edge of the soft dorsal fin and the leading edge of the tail during steady swimming at 1.0 L s^{-1}. (E) Corresponding plot of dorsal and caudal fin motion *versus* time for approximately two fin beat cycles showing that mediolateral oscillation of the tail is approximately one-quarter cycle out of phase with that of the dorsal fin. (F) Path of the caudal fin's leading edge (red dots) plotted over the course of one tail beat cycle and shown in relation to the wake of the dorsal fin within the frontal (*XY*) plane (position 2, Fig. 1A) at 1.0 L s^{-1}. At this speed, the tail passes directly through the centers of the dorsal fin vortices and experiences an incident flow whose velocity exceeds that of the free-stream by 3%. Free-stream velocity of 18.0 cm s^{-1} has been subtracted from the vector field.

and Videler, 1974; Jayne et al., 1996; Winterbottom, 1974). Electromyographic recordings from the dorsal inclinator muscles of bluegill sunfish reveal discrete activity patterns during both steady and unsteady swimming behaviors (Jayne et al., 1996). Although the recording of such activity has not yet been attempted for other species, we expect that the dorsal fin of trout also has the capacity to serve as an active control surface during locomotion. On the basis of observed locomotor kinematics, we may infer the extent to which the dorsal fin indeed moves as a result of independent muscular control. If the dorsal inclinator muscles were inactive during steady forward swimming, then lateral movement of the body would cause passive deflection of the dorsal fin in the opposite direction (Jayne et al., 1996). In this scenario, one would expect a substantial phase lag in the oscillatory motion of the dorsal fin and body (i.e. the maximal lateral excursion of the dorsal fin tip during each half-stroke would be delayed relative to that of the body at the same longitudinal position). Since this phase lag is negligible in trout (Fig. 3A,C,E), we predict that the dorsal inclinator muscles are active during rectilinear locomotion, functioning minimally to stiffen the dorsal fin and resist its tendency to bend passively as the body sweeps laterally through the water. If the inclinators served only to stiffen the dorsal fin, however, one would expect that the amplitude of side-to-side motion of the fin and body would be nearly identical. Although this pattern is seen for the adipose fin (Fig. 3B,D,F), which lacks intrinsic musculature, the dorsal fin's stroke amplitude exceeds that of the body at all but the

highest speed studied (Fig. 3A,C,E). In addition, during turning maneuvers, the dorsal fin is capable of extreme flexion (Figs 2F, 7) at any point during the body's undulatory period. We predict therefore that the dorsal fin of trout is under active muscular control during both steady and unsteady swimming, which allows the fin to act as a propulsor independent of the underlying body. This prediction may be tested in future work through electromyographic recording from the dorsal inclinators and observation of locomotor kinematics following chronic paralyzation of fin musculature.

Hydrodynamic function of the trout dorsal fin

Functions traditionally ascribed to the dorsal fin of basal teleost fishes have been largely non-propulsive. In the sister group to Teleostei, the highly elongate, undulatory dorsal fin of amiiform fishes plays a definitive role in thrust production during locomotion (Breder, 1926). However, the plesiomorphic teleostean dorsal fin, which has a short base of attachment to the body, has been regarded as serving more hydrodynamically passive roles, such as acting as a static keel or body stabilizer during rectilinear swimming and as a fixed pivot point for body rotation during turning maneuvers (Aleev, 1969; Harris, 1936). These proposed functions have persisted in the literature (Helfman et al., 1997, p. 168) in the absence of experimental data. Using kinematic analysis together with quantitative flow visualization, we test the hypothesis that the basal teleost dorsal fin morphology typified by trout plays a non-propulsive role in steady and unsteady locomotion.

The impact of an oscillating body on wake structure and associated fluid force is predicted by the Strouhal number, *St* (defined in Materials and methods). Experimental studies of foils in steady forward motion and a combination of heaving and pitching motion (Anderson, 1996; Anderson et al., 1998) reveal that when $St<0.2$, a loosely organized wake forms that generates very low or negative thrust. In this case, one observes either a 'wavy wake' with no distinct vortex formation or a drag-producing Kármán street characterized by staggered, counter-rotating vortices and a central region of jet flow oriented upstream that reduces the momentum of the incident flow. As *St* rises to within the range of 0.2–0.5, wake structure and force change dramatically: a reverse Kármán street develops that generates a strong thrust force (Anderson et al., 1998). This wake trail is comprised of paired vortices with opposite-sign rotation and a downstream-directed momentum jet between each vortex pair (Lighthill, 1975; Triantafyllou et al., 1993, 2000; von Kármán and Burgers, 1935; Weihs, 1972). Aside from a recent study of dorsal fin function in sunfish (Drucker and Lauder, 2001a), only the tail has been considered previously in calculations of median-fin Strouhal number. For rainbow trout, tail *St* shows a general decline with increasing swimming speed (Triantafyllou et al., 1993; based on calculations from Webb et al., 1984); similar results have been obtained for eels (Tytell, 2004). In the present study, we find a reduction in mean *St* for the oscillating dorsal fin of trout from 0.37 to 0.21 as speed increases from $0.5\,L\,s^{-1}$ (mean 9.8 cm s^{-1}) to $1.0\,L\,s^{-1}$ (mean 19.6 cm s^{-1}) (Table 2). This reduction in *St* to the lower limit of the range of predicted peak propulsive efficiency is reflected by a decrease in dorsal fin beat amplitude as speed increases to $1.0\,L\,s^{-1}$ (Fig. 3A,C). On the basis of these kinematic results, we reject the hypothesis presented above and predict that dorsal fin oscillation in trout over low to intermediate swimming speeds contributes to overall fluid force production for locomotion.

Further evidence to support this prediction comes from analysis of dorsal fin wake patterns in trout, which show a small but significant downstream (thrust) component of the central vortex jets (Table 2; Figs 4, 5). The dorsal fin of trout generates approximately 7.7% of the thrust generated by the tail at a swimming speed of $1.0\,L\,s^{-1}$. However, the most remarkable aspect of trout dorsal-fin hydrodynamic function is the large lateral forces generated by the dorsal fin at all swimming speeds at which a significant wake is observed. The trout dorsal fin generates five to six times as much laterally directed force as thrust, and the central vortex jet is directed at a mean angle of 75° to the body (Table 2). Comparative studies of the hydrodynamic function of fish fins have shown that the existence of a large lateral component of fin forces appears to be a general phenomenon (Drucker and Lauder, 1999, 2002b; Lauder and Drucker, 2002; Lauder et al., 2003). But no other median fin in any behavior studied to date has shown the extreme lateral force orientation exhibited by the trout dorsal fin. The occurrence of such lateral forces during routine rectilinear swimming clearly indicates that locomotion previously considered to be controlled exclusively by the body and caudal fin also involves significant anterior median fin activity. The possible impact that dorsal fin forces have on the overall force balance during locomotion is considered further below.

Comparisons to sunfish dorsal fin function

We have previously analyzed the dorsal fin wake in sunfish using techniques and swimming speeds directly comparable to those of this study (Drucker and Lauder, 2001a). Sunfish, unlike trout, possess an anterior spiny portion of the dorsal fin that supports the posterior soft-rayed section (Fig. 1). During steady swimming at approximately $1\,L\,s^{-1}$, the sunfish soft dorsal fin contributes 12.1% of the total thrust force generated by the median and paired fins. At this speed, the lateral component of dorsal fin force is twice the thrust force component, and the mean jet angle is 62°. In both trout and sunfish, then, the soft dorsal fin plays a significant role in steady propulsion and generates a large lateral force with each fin beat (Fig. 8B,D). However, in trout, this lateral force is approximately three times greater, relative to thrust force, than in sunfish. This proportionately greater lateral force generated by trout dorsal fins may be a function of the elongate, roughly cylindrical body shape of trout, a morphology with a greater susceptibility to roll than the gibbose and laterally flattened shape of sunfish. The soft dorsal fin must thus be viewed as an integral part of routine swimming in teleost fishes, generating both thrust and lateral (stabilizing) forces with each locomotor stroke cycle. Steady locomotion, at least in the species studied

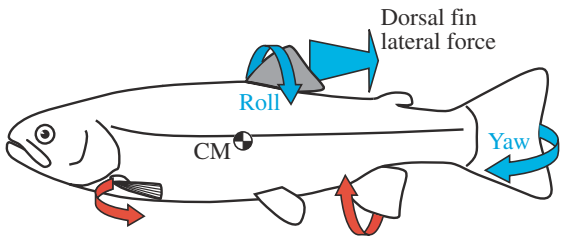

Fig. 10. Schematic illustration of laterally directed dorsal fin force (large blue arrow) generated during steady swimming at 0.5 and 1.0 $L\ s^{-1}$ by rainbow trout, the roll and yaw torques (curved blue arrows) induced by this dorsal fin moment, and the hypothesized counteracting torques (red arrows) produced by the pectoral and anal fins to achieve a moment balance during steady locomotion. Asymmetrical movement of the caudal fin and oscillation of the pelvic fins could also assist in generating compensatory roll and yaw moments. Although the paired fins are not recruited continuously by trout during steady swimming (Drucker and Lauder, 2003), intermittent excursions of these propulsors may serve to correct moment imbalances. Steady swimming by trout involves the active use of multiple fins to maintain body stability in the face of environmental perturbations. CM, center of mass of the body.

to date, necessarily involves force generation both by the dorsal fin and by the body and caudal fin.

These large lateral forces have important implications for the overall force balance in swimming fishes. Lateral forces generated by the soft dorsal fin are transmitted to the body along the area of attachment of the dorsal fin. This attachment site is located above the center of mass of the body in both sunfish and trout (Fig. 10; see also fig. 5 in Drucker and Lauder, 2002b), and therefore lateral force production will induce a roll moment. In addition, the middle of the broad dorsal fin attachment is located posterior to the body's center of mass, and hence lateral dorsal fin force will induce a yaw moment. For fishes to swim steadily forward with minimal roll and yaw, other fins must counteract these moments, including the anal fin, caudal fin, pectoral fins and possibly also the pelvic fins (Fig. 10), whose locomotor function in freely swimming fishes is poorly understood. The anal and caudal fins may exert compensatory torques continuously during their oscillatory motions, while the paired fins, which are not oscillated regularly during steady swimming in trout (Drucker and Lauder, 2003), may instead act intermittently to correct moment imbalances. Under this view of fish propulsion, nearly all fins are involved in body stabilization, especially at low speeds, and in the overall force balance during steady rectilinear propulsion. Oscillation of multiple fins with substantial kinematic phase delay, as observed for the dorsal and caudal fins in trout (Fig. 9E), produces multiple discrete forces during each locomotor cycle, a mechanism predicted to be in widespread use among teleost fishes for relatively constant thrust generation over time (cf. Arreola and Westneat, 1996).

The roll moment induced by dorsal fin activity in trout leads to a prediction about the function of the anal fin that is amenable to experimental test. Since the attachment of the anal fin is ventral to the body's center of mass, anal fin wake flow is expected to contain vortex structures that produce lateral jet flows to the *same* side of the body as those of the dorsal fin. Same-side jet flows would result in *opposing* torques and contribute to a balance of roll forces. Based on the results of this study, we suggest that the distinction between MPF propulsion and BCF propulsion in fishes obscures the important role of multiple propulsors, including the tail and other median fins, which act in a coordinated fashion to stabilize the body during steady rectilinear locomotion (also see Lauder, 2005).

In sunfish, we demonstrated previously that the tail passes through the wake of the dorsal fin and experiences an altered hydrodynamic environment relative to free-stream flow (Drucker and Lauder, 2001a). Depending on the structure of this wake, the kinematic phase lag between caudal and dorsal fins and the relative amplitudes of lateral motion, the caudal fin could experience enhanced thrust as a result of intercepting dorsal fin vortices. During steady swimming at low speed, the tail of sunfish moves through a staggered array of dorsal fin vortices whose rotational flow is hypothesized to increase incident velocity over the tail and to enhance same-sign vorticity bound to the tail (see figs 7, 10 in Drucker and Lauder, 2001a). In trout, the dorsal fin wake trail at 1 $L\ s^{-1}$ is generally similar to that of sunfish, taking the form of a reverse Kármán street (Fig. 8B,D). Vortices within the trout dorsal fin wake, however, are more linearly arranged than in the wake of sunfish; hence, sinusoidal excursions of the trout tail cut through the vortex centers left behind the dorsal fin (Fig. 9F). During steady swimming at 1 $L\ s^{-1}$, the tail encounters a dorsal fin wake flow with a downstream component increased over free-stream flow velocity by an average of 35% and 3%, respectively, in sunfish and trout. This increased velocity could theoretically augment drag forces but, depending on the phase and angle of tail motion relative to the incident flow, may instead reinforce developing circulation around the tail or enhance attached separation of the tail's leading-edge vortex (cf. Akhtar and Mittal, 2005; Mittal, 2004) and thereby enhance overall tail thrust production.

A number of recent experimental studies of foils heaving and pitching in a variety of wake flow patterns have addressed the effect of foil–flow interactions on foil thrust and efficiency (Anderson, 1996; Beal, 2003; Lewin and Haj-Hariri, 2003; Read et al., 2003; Triantafyllou et al., 1993, 2000). Although most of these studies have focused on foils encountering drag wakes, several important conclusions have emerged that are relevant to understanding possible hydrodynamic interactions between the caudal and dorsal fins. Thrust generated by foils encountering an oscillating incident flow is maximized when there is a phase lag of ~100° between the foil and the flow. At this phase difference, lateral motion of the foil's leading edge is opposed by lateral motion of the oncoming fluid (Beal, 2003). This increases the effective angle of attack of the foil. In addition, motion of the foil's leading edge in opposition to oncoming flow may increase the duration of leading-edge

vortex attachment to the tail fin, delaying stall and hence increasing mean lift force over the duration of a tail beat. Enhancement of mean circulation could also occur as a result of increased flow velocity over the tail. Fig. 9E,F shows that the tail of trout undergoes lateral motions that are phase-delayed relative to, and directly opposed by, lateral flows generated by the dorsal fin in the manner described by Beal (2003) for foils generating peak thrust. Understanding the precise effect of incident wake structure on tail thrust magnitude awaits detailed visualizations of fluid motion on the tail surface and computational studies of thrust calculated from flow structure and tail and dorsal fin kinematics. But existing experimental data from both trout and sunfish demonstrate that the caudal fin, when oscillating in tandem with the dorsal fin, experiences a flow environment that is markedly different from the free-stream flow lateral to the fish body.

Comparison of dorsal fin function in sunfish and trout additionally reveals that the species differ considerably in the magnitude of locomotor force generated per unit dorsal fin area, with trout generating substantially smaller relative forces. During steady swimming at 1 $L\ s^{-1}$, the sunfish soft dorsal fin generates 6.3 times more thrust and 2.4 times more lateral force per unit fin area than the trout dorsal fin. During slow turning, sunfish exert 65 times more thrust per area and 3.6 times more lateral force per area than trout (Table 2; fig. 20 in Lauder and Drucker, 2004).

Functional design of fish median fins

Significant evolutionary changes in median fin structure within ray-finned fishes have resulted in a diversity of dorsal, anal and caudal fin configurations (Drucker and Lauder, 2001a; Lauder and Liem, 1983; Rosen, 1982). Five key areas of diversity in median fin design are (1) the presence or absence of an anterior spiny dorsal fin, (2) the extent of separation of the spiny and soft dorsal fins (the two can be widely separated or attached, as in sunfish), (3) the distance between the trailing dorsal fin margin and the leading edge of the caudal fin, (4) the size and kinematic versatility of the anal fin and (5) the presence or absence of an adipose fin on the dorsal midline. Empirical quantitative data on dorsal fin hydrodynamic function are only available for two species to date (trout and sunfish), and it is thus premature to speculate on broader functional patterns. But current wake visualization data do lead to a number of hypotheses regarding the functional design of median fins that could be tested through future experimental and computational hydrodynamic studies in a broader array of species.

First, the propulsive force generated by the dorsal fin per unit fin area is expected to be greater in species with a dorsal fin design like that of sunfish as opposed to that of trout. Stabilization of the leading edge of the soft dorsal fin by anterior spiny elements (Fig. 1B) may permit more rapid lateral fin motion around the soft dorsal fin's leading edge and larger momentum transfers to the water. Without leading-edge stabilization, soft dorsal fin musculature may be required to stiffen the fin substantially in addition to providing force for lateral oscillation. Coactivation of right- and left-side inclinator muscles for soft dorsal fin stiffening may greatly reduce the magnitude of fin force per unit area that can be generated for propulsion.

Second, constructive hydrodynamic interactions among median fins may be more prevalent in species with more closely apposed fins. Vortices shed by the soft dorsal fin carry fluid energy downstream, which may be absorbed by the tail to augment thrust according to the tail's proximity to and phase relationship with the upstream propulsor. When the distance between the trailing edge of the soft dorsal fin and the leading edge of the tail is relatively small, as in short-bodied species like sunfish (Fig. 1B), dorsal fin vortices encountered by the tail can enhance circulation around the tail and potentially augment caudal fin thrust (Drucker and Lauder, 2001a). By contrast, when this inter-fin distance is relatively large, as in elongate fishes like trout (Fig. 1A), the energy of dorsal fin vortices may be reduced by the time these wake structures are intercepted by the tail so that constructive hydrodynamic interactions are much less likely.

Third, the anal fin should exhibit in-phase movement with the dorsal fin (i.e. simultaneous ipsilateral excursion) in species subject to roll moments around the body's center of mass resulting from laterally directed dorsal fin forces (Fig. 10). A recent kinematic analysis of dorsal and anal fin motion in sunfish (Standen and Lauder, 2005) supports this hypothesis. Experiments simultaneously quantifying the wake of dorsal and anal fins in a variety of species would further clarify functional interdependencies between these median fins.

Finally, the enigmatic adipose fin present in many euteleostean fishes (Fig. 1A) remains of uncertain function. Data presented here confirm that it shows negligible movement independent of the body, but wake visualization does clearly reveal a narrow, sinusoidal drag wake downstream of the adipose fin that is intercepted by the tail. The hydrodynamic function of such a drag wake remains incompletely understood, particularly in regard to its effect on flow at the tail surface. On the basis of computational studies of tandem flapping foils (Akhtar and Mittal, 2005; Mittal, 2004), we speculate that the adipose fin's drag wake influences the flow environment around the caudal fin, causing an augmentation of thrust through enhancement of the tail's leading-edge vortex. This hypothesis is probably best addressed *via* a combination of computational fluid dynamic simulations of flow over the tail and direct measurement of forces on a tandem pair of computer-controlled heaving and pitching foils undergoing realistic median fin motions. Reimchen and Temple (2004) have recently shown that in some trout the tail beat amplitude increases (mean 8%) when the adipose fin is removed. This apparent functional compensation by the tail points towards a definitive role of the adipose fin in locomotor force production. The adipose fin, present in so many euteleostean fishes, remains an intriguing aspect of median fin design deserving of additional study.

We thank Laura Farrell for assistance in maintaining fish and for helping with experiments, Adam Summers and two

anonymous referees for constructive comments on the manuscript, and Danny Backenroth for developing circulation and wake jet analysis software. E.G.D. expresses gratitude to Kelly Overly for her continuing forbearance. Supported by NSF grants DBI-9750321 to E.G.D. and IBN-0316675 to G.V.L.

References

Akhtar, I. and Mittal, R. (2005). A biologically inspired computational study of flow past tandem flapping foils. *AIAA J.* **4760**, 1-12.

Aleev, Y. G. (1969). *Function and Gross Morphology in Fish*. Jerusalem: Keter Press. (translated from the Russian by M. Raveh.)

Anderson, J. (1996). Vorticity control for efficient propulsion. PhD thesis, Massachusetts Institute of Technology/Woods Hole Oceanographic Institution, Cambridge, MA, USA.

Anderson, J. M., Streitlein, K., Barrett, D. S. and Triantafyllou, M. S. (1998). Oscillating foils of high propulsive efficiency. *J. Fluid Mech.* **360**, 41-72.

Arreola, V. I. and Westneat, M. W. (1996). Mechanics of propulsion by multiple fins: kinematics of aquatic locomotion in the burrfish (*Chilomycterus schoepfi*). *Proc. R. Soc. Lond. B* **263**, 1689-1696.

Beal, D. N. (2003). Propulsion through wake synchronization using a flapping foil. PhD thesis, Massachusetts Institute of Technology/Woods Hole Oceanographic Institution, Cambridge, MA, USA.

Blake, R. W. (1976). On seahorse locomotion. *J. Mar. Biol. Assoc. UK* **56**, 939-949.

Blake, R. W. (1977). On ostraciiform locomotion. *J. Mar. Biol. Assoc. UK* **57**, 1047-1055.

Blake, R. W. (1978). On balistiform locomotion. *J. Mar. Biol. Assoc. UK* **58**, 73-80.

Blake, R. W. (1980). Undulatory median fin propulsion of two teleosts with different modes of life. *Can. J. Zool.* **58**, 2116-2119.

Breder, C. M., Jr (1926). The locomotion of fishes. *Zoologica* **4**, 159-296.

Breder, C. M., Jr and Edgerton, H. E. (1942). An analysis of the locomotion of the seahorse, *Hippocampus*, by means of high speed cinematography. *Ann. NY Acad. Sci.* **43**, 145-172.

Consi, T. R., Seifert, P. A., Triantafyllou, M. S. and Edelman, E. R. (2001). The dorsal fin engine of the seahorse (*Hippocampus* sp.). *J. Morphol.* **248**, 80-97.

Dickinson, M. H. (1996). Unsteady mechanisms of force generation in aquatic and aerial locomotion. *Am. Zool.* **36**, 537-554.

Dickinson, M. H. and Götz, K. G. (1996). The wake dynamics and flight forces of the fruit fly *Drosophila melanogaster*. *J. Exp. Biol.* **199**, 2085-2104.

Drucker, E. G. and Lauder, G. V. (1999). Locomotor forces on a swimming fish: three-dimensional vortex wake dynamics quantified using digital particle image velocimetry. *J. Exp. Biol.* **202**, 2393-2412.

Drucker, E. G. and Lauder, G. V. (2000). A hydrodynamic analysis of fish swimming speed: wake structure and locomotor force in slow and fast labriform swimmers. *J. Exp. Biol.* **203**, 2379-2393.

Drucker, E. G. and Lauder, G. V. (2001a). Locomotor function of the dorsal fin in teleost fishes: experimental analysis of wake forces in sunfish. *J. Exp. Biol.* **204**, 2943-2958.

Drucker, E. G. and Lauder, G. V. (2001b). Wake dynamics and fluid forces of turning maneuvers in sunfish. *J. Exp. Biol.* **204**, 431-442.

Drucker, E. G. and Lauder, G. V. (2002a). Experimental hydrodynamics of fish locomotion: functional insights from wake visualization. *Integ. Comp. Biol.* **42**, 243-257.

Drucker, E. G. and Lauder, G. V. (2002b). Wake dynamics and locomotor function in fishes: interpreting evolutionary patterns in pectoral fin design. *Integ. Comp. Biol.* **42**, 997-1008.

Drucker, E. G. and Lauder, G. V. (2003). Function of pectoral fins in rainbow trout: behavioral repertoire and hydrodynamic forces. *J. Exp. Biol.* **206**, 813-826.

Geerlink, P. J. and Videler, J. J. (1974). Joints and muscles of the dorsal fin of *Tilapia nilotica* L. (Fam. Cichlidae). *Neth. J. Zool.* **24**, 279-290.

Gordon, M. S., Hove, J. R., Webb, P. W. and Weihs, D. (2000). Boxfishes as unusually well-controlled autonomous underwater vehicles. *Physiol. Biochem. Zool.* **73**, 663-671.

Gosline, W. A. (1971). *Functional Morphology and Classification of Teleostean Fishes*. Honolulu: University of Hawaii Press.

Harris, J. E. (1936). The role of the fins in the equilibrium of the swimming fish. I. Wind tunnel tests on a model of *Mustelus canis* (Mitchell). *J. Exp. Biol.* **13**, 476-493.

Harris, J. E. (1937). The mechanical significance of the position and movements of the paired fins in the Teleostei. *Pap. Tortugas Lab.* **31**, 173-189.

Hart, D. P. (1998). High-speed PIV analysis using compressed image correlation. *ASME J. Fluids Eng.* **120**, 463-470.

Helfman, G. S., Collette, B. B. and Facey, D. E. (1997). *The Diversity of Fishes*. Malden, Massachusetts: Blackwell Science.

Hove, J. R., O'Bryan, L. M., Gordon, M. S., Webb, P. W. and Weihs, D. (2001). Boxfishes (Teleostei: Ostraciidae) as a model system for fishes swimming with many fins: kinematics. *J. Exp. Biol.* **204**, 1459-1471.

Jayne, B. C., Lozada, A. and Lauder, G. V. (1996). Function of the dorsal fin in bluegill sunfish: motor patterns during four locomotor behaviors. *J. Morphol.* **228**, 307-326.

Kalleberg, H. (1958). Observations in a stream tank of territoriality and competition in juvenile salmon and trout (*Salmo salar* L. and *S. trutta* L.). *Rep. Inst. Freshwat. Res. Drottningholm* **39**, 55-98.

Keenleyside, M. H. A. and Yamamoto, F. T. (1962). Territorial behaviour of juvenile Atlantic salmon (*Salmo salar* L.). *Behaviour* **19**, 139-169.

Korsmeyer, K. E., Steffensen, J. F. and Herskin, J. (2002). Energetics of median and paired fin swimming, body and caudal fin swimming, and gait transition in parrotfish (*Scarus schlegeli*) and triggerfish (*Rhinecanthus aculeatus*). *J. Exp. Biol.* **205**, 1253-1263.

Lauder, G. V. (2000). Function of the caudal fin during locomotion in fishes: kinematics, flow visualization, and evolutionary patterns. *Am. Zool.* **40**, 101-122.

Lauder, G. V. (2005). Locomotion. In *The Physiology of Fishes*, 3rd edn (ed. D. H. Evans and J. B. Claiborne), pp. 3-46. Boca Raton: CRC Press.

Lauder, G. V. and Drucker, E. G. (2002). Forces, fishes, and fluids: hydrodynamic mechanisms of aquatic locomotion. *News Physiol. Sci.* **17**, 235-240.

Lauder, G. V. and Drucker, E. G. (2004). Morphology and experimental hydrodynamics of fish fin control surfaces. *IEEE J. Ocean. Eng.* **29**, 556-571.

Lauder, G. V. and Liem, K. F. (1983). The evolution and interrelationships of the actinopterygian fishes. *Bull. Mus. Comp. Zool.* **150**, 95-197.

Lauder, G. V., Nauen, J. C. and Drucker, E. G. (2002). Experimental hydrodynamics and evolution: function of median fins in ray-finned fishes. *Integ. Comp. Biol.* **42**, 1009-1017.

Lauder, G. V., Drucker, E. G., Nauen, J. C. and Wilga, C. D. (2003). Experimental hydrodynamics and evolution: caudal fin locomotion in fishes. In *Vertebrate Biomechanics and Evolution* (ed. V. Bels, J.-P. Gasc and A. Casinos), pp. 117-135. Oxford: BIOS Scientific Publishers.

Lewin, G. C. and Haj-Hariri, H. (2003). Modelling thrust generation of a two-dimensional heaving airfoil in a viscous flow. *J. Fluid Mech.* **492**, 339-362.

Liao, J. C. and Lauder, G. V. (2000). Function of the heterocercal tail in white sturgeon: flow visualization during steady swimming and vertical maneuvering. *J. Exp. Biol.* **203**, 3585-3594.

Liao, J. C., Beal, D. N., Lauder, G. V. and Triantafyllou, M. S. (2003a). Fish exploiting vortices decrease muscle activity. *Science* **302**, 1566-1569.

Liao, J. C., Beal, D. N., Lauder, G. V. and Triantafyllou, M. S. (2003b). The Kármán gait: novel body kinematics of rainbow trout swimming in a vortex street. *J. Exp. Biol.* **206**, 1059-1073.

Lighthill, J. and Blake, R. (1990). Biofluiddynamics of balistiform and gymnotiform locomotion. Part 1. Biological background and analysis by elongated-body theory. *J. Fluid Mech.* **212**, 183-207.

Lighthill, M. J. (1975). *Mathematical Biofluiddynamics*. Philadelphia: Society for Industrial and Applied Mathematics.

Lindsey, C. C. (1978). Form, function, and locomotory habits in fish. In *Fish Physiology*, vol. VII (ed. W. S. Hoar and D. J. Randall), pp. 1-100. New York: Academic Press.

Lissmann, H. W. (1961). Zoology, locomotory adaptations and the problem of electric fish. In *The Cell and the Organism* (ed. J. A. Ramsay and V. B. Wigglesworth), pp. 301-317. London: Cambridge University Press.

Mabee, P. M., Crotwell, P. L., Bird, N. C. and Burke, A. C. (2002). Evolution of median fin modules in the axial skeleton of fishes. *J. Exp. Zool.* **294**, 77-90.

McLaughlin, R. L. and Noakes, D. L. G. (1998). Going against the flow: an examination of the propulsive movements made by young brook trout in streams. *Can. J. Fish. Aquat. Sci.* **55**, 853-860.

Milne-Thomson, L. M. (1966). *Theoretical Aerodynamics*, 4th edn. New York: Macmillan.

Mittal, R. (2004). Computational modeling in biohydrodynamics: trends, challenges, and recent advances. *IEEE J. Ocean. Eng.* **29**, 595-604.

Nauen, J. C. and Lauder, G. V. (2002a). Hydrodynamics of caudal fin locomotion by chub mackerel, *Scomber japonicus* (Scombridae). *J. Exp. Biol.* **205**, 1709-1724.

Nauen, J. C. and Lauder, G. V. (2002b). Quantification of the wake of rainbow trout (*Oncorhynchus mykiss*) using three-dimensional stereoscopic digital particle image velocimetry. *J. Exp. Biol.* **205**, 3271-3279.

Read, D. A., Hover, F. S. and Triantafyllou, M. S. (2003). Forces on oscillating foils for propulsion and maneuvering. *J. Fluids Struct.* **17**, 163-183.

Reimchen, T. E. and Temple, N. F. (2004). Hydrodynamic and phylogenetic aspects of the adipose fin in fishes. *Can. J. Zool.* **82**, 910-916.

Rosen, D. E. (1982). Teleostean interrelationships, morphological function, and evolutionary inference. *Am. Zool.* **22**, 261-273.

Spedding, G. R., Rayner, J. M. V. and Pennycuick, C. J. (1984). Momentum and energy in the wake of a pigeon (*Columba livia*) in slow flight. *J. Exp. Biol.* **111**, 81-102.

Standen, E. M. and Lauder, G. V. (2005). Dorsal and anal fin function in bluegill sunfish *Lepomis macrochirus*: three-dimensional kinematics during propulsion and maneuvering. *J. Exp. Biol.* **208**, 2753-2763.

Triantafyllou, G. S., Triantafyllou, M. S. and Grosenbaugh, M. A. (1993). Optimal thrust development in oscillating foils with application to fish propulsion. *J. Fluids Struct.* **7**, 205-224.

Triantafyllou, M. S., Triantafyllou, G. S. and Yue, D. K. P. (2000). Hydrodynamics of fishlike swimming. *Annu. Rev. Fluid Mech.* **32**, 33-53.

Tytell, E. D. (2004). The hydrodynamics of eel swimming. II. Effect of swimming speed. *J. Exp. Biol.* **207**, 3265-3279.

von Kármán, T. and Burgers, J. M. (1935). General aerodynamic theory. Perfect fluids. In *Aerodynamic Theory*, vol. 2 (ed. W. F. Durand), p. 308. Berlin: Springer-Verlag.

Webb, P. W. (1971). The swimming energetics of trout. I. Thrust and power output at cruising speeds. *J. Exp. Biol.* **55**, 489-520.

Webb, P. W. (1984). Body form, locomotion and foraging in aquatic vertebrates. *Am. Zool.* **24**, 107-120.

Webb, P. W. (1991). Composition and mechanics of routine swimming of rainbow trout, *Oncorhynchus mykiss*. *Can. J. Fish. Aquat. Sci.* **48**, 583-590.

Webb, P. W. (1994). Exercise performance of fish. In *Advances in Veterinary Science and Comparative Medicine*, vol. 38B (ed. J. H. Jones), pp. 1-49. San Diego: Academic Press.

Webb, P. W. and Gardiner Fairchild, A. (2001). Performance and maneuverability of three species of teleostean fishes. *Can. J. Zool.* **79**, 1866-1877.

Webb, P. W. and Gerstner, C. L. (2000). Fish swimming behaviour: predictions from physical principles. In *Biomechanics in Animal Behaviour* (ed. P. Domenici and R. W. Blake), pp. 59-77. Oxford: BIOS Scientific Publishers.

Webb, P. W., Kostecki, P. T. and Stevens, E. D. (1984). The effect of size and swimming speed on the locomotor kinematics of rainbow trout. *J. Exp. Biol.* **109**, 77-95.

Weihs, D. (1972). Semi-infinite vortex trails, and their relation to oscillating airfoils. *J. Fluid Mech.* **54**, 679-690.

Willert, C. E. and Gharib, M. (1991). Digital particle image velocimetry. *Exp. Fluids* **10**, 181-193.

Winterbottom, R. (1974). A descriptive synonymy of the striated muscles of the Teleostei. *Proc. Acad. Nat. Sci. Phila.* **125**, 225-317.

Wolfgang, M. J., Anderson, J. M., Grosenbaugh, M., Yue, D. and Triantafyllou, M. (1999). Near-body flow dynamics in swimming fish. *J. Exp. Biol.* **202**, 2303-2327.

Wright, B. (2000). Form and function in aquatic flapping propulsion: morphology, kinematics, hydrodynamics, and performance of the triggerfishes (Tetraodontiformes: Balistidae). Ph.D. Thesis, University of Chicago.